Temperature dependent phonon renormalization in metallic nanotubes

V. Scardaci[1], S. Piscanec[1], Michele Lazzeri[2], R. Krupke[3], Francesco Mauri[2],* and A.C. Ferrari[1†]
[1] *Cambridge University, Engineering Department, 9 JJ Thomson Avenue, Cambridge CB3 OFA, United Kingdom*
[2] *Institut de Mineralogie et de Physique des Milieux Condenses, Paris, France*
[3] *Institut für Nanotechnologie Forschungszentrum Karlsruhe, Germany*
(Dated: February 2, 2008)

We measure the temperature dependence of the Raman spectra of metallic and semiconducting nanotubes. We show that the different trend in metallic tubes is due to phonon re-normalization induced by the variation in electronic temperature, which is modeled including non-adiabatic contributions to account for the dynamic, time dependent nature of the phonons.

Raman spectroscopy is a powerful non destructive technique for the characterization of carbon materials, and is a fundamental tool in the recent advances in the understanding of single wall carbon nanotubes (SWNTs). Raman experiments probe the optical phonons, allowing to assess the vibrational properties of the analyzed materials. A strong interplay exists between temperature (T) and phonon frequencies. Indeed, because of anharmonic effects in the atomic oscillations, an increase in T usually results in a downshift of the phonon energy and a lifetime reduction [1]. For Raman active modes, this corresponds to a downshift and a broadening of the Raman peaks [1].

The temperature dependence of the Raman spectra is extremely effective for the evaluation of the local heating in a variety of electronic devices [2, 3], and provides valuable information for the characterization of nanomaterials [4]. Since SWNTs are at the center of nanotechnology research, a thorough investigation and understanding of the temperature effects on their Raman spectra is needed, especially in view of their foreseen application in high current nanodevices. Several groups reported changes of the Raman spectra of single-, double- and multi-wall tubes as a function of T. Some focussed on the G band [5, 6, 7, 8, 9, 10, 11, 12, 13]. Others considered the position [5, 6, 7, 8, 11, 12, 14] and the intensity [14] of the Radial Breathing Modes (RBM). A few reported the temperature evolution of the 2D [5, 13] and 2D' modes [5].

However, the different components of the G band, which crucially distinguish metallic from semiconducting nanotubes, were not independently studied, in order to ascertain if those would have a different temperature evolution in semiconducting and metallic SWNTs, thus fingerprinting each material.

Here we present an extensive set of temperature-dependent measurements of the G^+ and G^- peaks in metallic and semiconducting SWNTs. We show that there is a significant difference in the measured trends. We detect a re-normalization of the G^- peak, ruled by the variation in the electronic temperature, in metallic SWNTs. Furthermore, we prove that this can only be explained by considering the dynamic nature of the phonons and the resulting breakdown of the Born-Oppenheimer approximation. The re-normalized phonon frequencies in the standard static approaches being in total disagreement with the experiments.

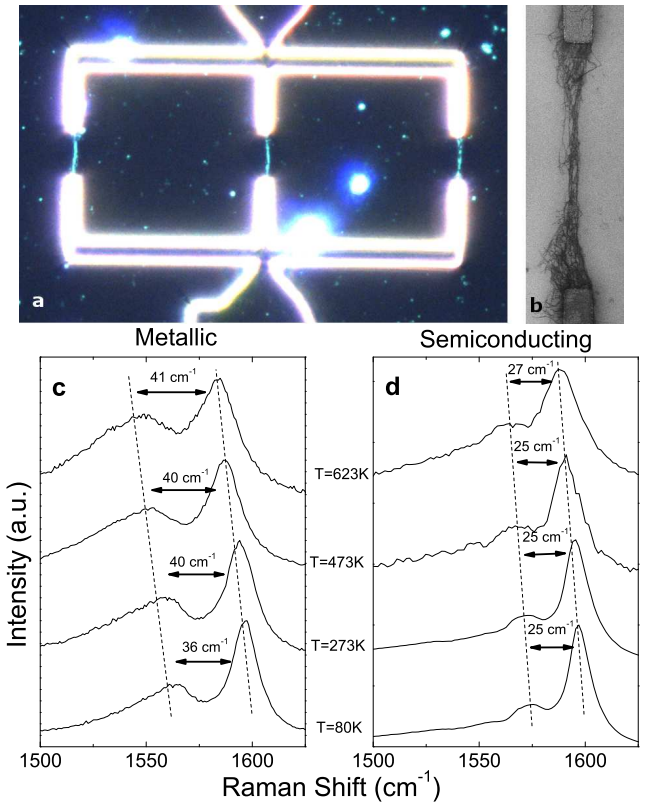

FIG. 1: (a) Dark-field microscopy image of the electrodes used in the dielectrophoretic deposition, (b) SEM image of the metallic tubes attached to the electrodes after dielectrophoresis and Raman spectra of (c) metallic and (d) semiconducting tubes acquired at T=80K, 273K, 473K and 623K.

Samples containing almost exclusively metallic SWNTs are prepared by depositing individually dispersed SWNT onto micro-electrodes using radio frequency dielectrophoresis as described in Ref. [15, 16]. The SWNT suspension is obtained by sonicating 100mL D_2O mixed with 0.05 weight % HiPCo-tube raw material provided by "Houston" and 1 weight % of sodium

dodecylbenzene sulfonate (SDBS) (Sigma-Aldrich). The suspension is centrifuged at 154000 g for 2 h and the upper 90% of the supernatant decanted. This is then diluted with D_2O to obtain a surfactant concentration of 0.1 weight % close to the critical micelle concentration (0.097 weight %). Microelectrodes with 10 μm gap are then produced from gold by standard electron beam lithography and bond-wired to a function generator. Dielectrophoretic deposition is conducted by exposing the electrodes driven at a frequency of 3 MHz and a peak-to-peak voltage V_{pp} of 20 V to a drop of suspension ($\sim$ 10μL). After 10 min the samples are subsequently rinsed with H_2O, ethanol and dried in nitrogen. They are then characterized by optical dark-field microscopy (Fig. 2a), electron microscopy (Fig. 2b) and Raman spectroscopy (Fig. 2c), which show that aligned bundles of metallic SWNTs bridge the electrodes.

Temperature dependent Raman measurements are carried out with a Renishaw 1000 spectrometer, using a He-Ne laser at 633 nm, matching the resonance window for HiPCo metallic tubes [17]. To further enhance the signal, the laser is polarized parallel to the aligned tubes. The temperature of the sample is set by a Linkam stage, in the range 77-850K. The stage is cooled by liquid N_2. Raman spectra are recorded from 80 to 630 K with steps of 25 K. From the RBM frequency [17, 18, 19] we estimate the mean diameter of metallic tubes to be $\sim$ 1.0 nm.

We also acquire spectra from samples with a natural mixture of metallic and semiconducting HiPCo-tubes. There we use 514 nm excitation, which brings semiconducting SWNTs with a diameter of $\sim$ 1.1 nm in resonance, as confirmed by the analysis of the RBMs. The semiconducting nature of the measured tubes is also confirmed by the shape and position of the G^--peak [20].

The G^+ and G^- peaks of metallic and semiconducting tubes measured at 80 K, 273 K, 473 K, and 625K are shown in Fig. 1. To quantitatively determine the peak positions, we fit the two components of the G band using 2 Lorentzians. An increasing temperature results in a downshift of both G^+ and G^-. This is in agreement with all previous observations [5, 6, 7, 8, 9, 10, 11, 12, 13] and can be explained by an-harmonicity. However, we crucially detect that in semiconducting tubes the splitting between G^+ and G^- is $\sim$ 25 cm^{-1}, independent of temperature, while in metallic it increases with T. This different behavior seems unlikely to originate from an-harmonicity.

The G^+ and G^- peaks originate from the tangential (TO) and the longitudinal (LO) modes derived from the splitting of the E_{2g} phonon of graphene. In metallic tubes, the LO mode is affected by a Kohn anomaly (KA) [21], which causes the softening of this phonon [20, 22]. Since KA are not present in semiconducting SWNTs, the G^+, G^- assignment in metallic SWNTs is the opposite of semiconducting tubes [20, 22].

For a given temperature and SWNT diameter, the softening of the LO mode in metallic with respect to semiconducting SWNTs originates from an anomalous screening of the atomic displacements, due to the electrons close to the Fermi energy. The occupation of these electronic states depends on temperature through the Fermi-Dirac distribution. Thus, in principle, changes in temperature may result in a modification of the electronic screening (see, for example, Ref. [23]), which can re-normalize the LO phonon frequency and the position of its corresponding Raman peak. This contribution, if present, would depend only on the electronic temperature T_e, and has to be added to the an-harmonic effects.

The influence of T_e on the screening of the atomic vibrations can be investigated theoretically. In general, lattice dynamics is calculated within the Born-Oppenheimer adiabatic framework [24, 25]. This assumes the motions of ions and electrons to be completely decoupled, with the electrons following adiabatically the ions (in other words, the electrons always "see" the ions as if they are in fixed positions). This is justified when the occupied and empty states are separated by an energy gap [26]. In materials without an electronic gap, the Born-Oppenheimer approximation (BOA) is not easily justifiable, however experience proves that in most cases this accurately reproduces the phonon dispersion of metals [27].

Phonon calculations within the BOA and based on zone-folding are in good agreement with room T Raman measurements of SWNTs [22]. However, we have shown that the BOA breaks down in the description of KA in doped graphene [28, 29]. Therefore, it is necessary to probe whether an adiabatic approach can reproduce the T evolution of the SWNTs Raman peaks.

Phonons can be regarded as a perturbation of a crystal [30]. In general, given their dynamic nature, they should be described by time-dependent perturbation theory (TDPT) [30]. However, within the adiabatic BOA, they are seen as static perturbations and treated by a time-independent perturbation theory (TIPT) [30].

Starting from the general expression given in Ref. [31] and following the approach described in Ref. [28], it can be shown that, within TDPT, the reciprocal-space expression for the non analytic part of the dynamical matrix of SWNTs, Θ_q is given by:

$$\tilde{\Theta}_q = \frac{4\tau A_{\Gamma/K}}{2\pi} \sum_{m,n=L,R} \int_{-\bar{k}}^{\bar{k}} |D_{(K+k'+q)n,(K+k')m}|^2 \frac{f_{K+k,m} - f_{K+k'+q,n}}{\epsilon_{K+k',m} - \epsilon_{K+k'+q,n} + \hbar\omega_q + i\gamma} dk', \quad (1)$$

where τ is the length of the translational unit cell of the tube, k' is measured from the Fermi point k_F; $\bar{k}$ has a small but finite value; R and L label the bands crossing at the Fermi energy and corresponding respectively to right- and left-moving electrons; $A_{\Gamma/K}$ accounts for the number of processes satisfying $2q = k_F$ ($A_\Gamma = 2$, $A_K = 1$),$\hbar\omega_q$ is the energy of a phonon of wavevector 4 and branch η

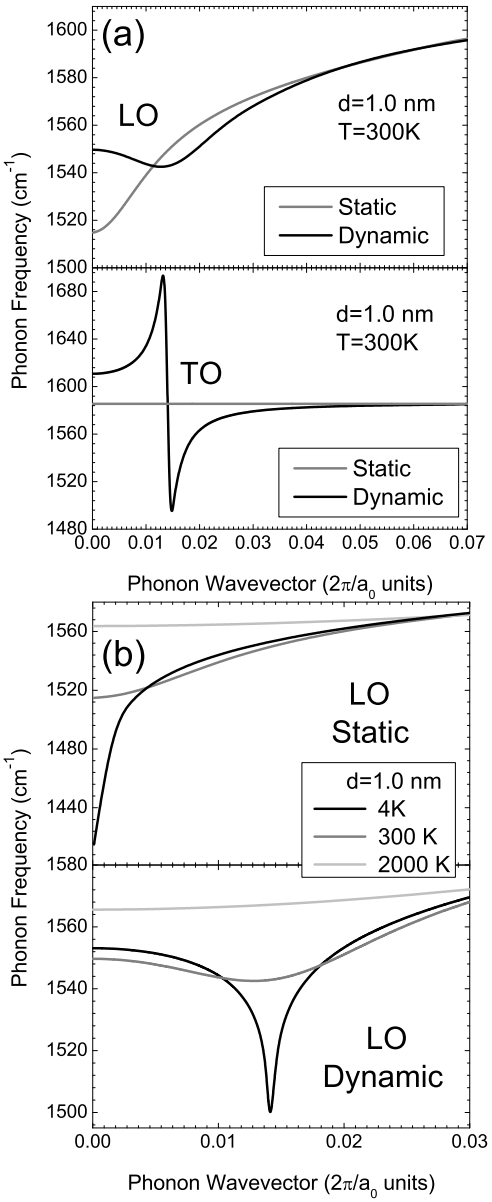

FIG. 2: (a)Comparison of the static and dynamic phonon dispersions of the LO and TO modes close to q=0. (b) Static and dynamic phonon dispersion of the LO mode close to q=0 calculated at T_e =4K, 300K, and 2000K.

(omitted in the equations for simplicity), γ is a small real number, $D_{(k+q)i,kj} = \langle k+q, i|\Delta V_q|k, j\rangle$ is the electron-phonon coupling (EPC) matrix element where $|k, i\rangle$ is the electronic Bloch eigenstate of wavevector k, band i, energy $\epsilon_{k,i}$, and occupation $f_{k,i}$ given by the Fermi-Dirac distribution [32]; ΔV_q is the derivative of the electronic potential with respect to the phonon normal coordinate.

Within the BOA, a phonon is seen in its static limit, i.e. assuming $\omega_q = 0$ and $\gamma = 0$. $\tilde{\Theta}_q$ thus simplifies in:

$$\tilde{\Theta}_{\rm q} = \frac{2A_{\Gamma/{\rm K}}T}{2\pi} \sum_{m,n=L,R} \int_{-\bar{k}}^{\bar{k}} \frac{f_{{\rm K+k'},m} - f_{{\rm K+k'+q},n}}{\epsilon_{{\rm K+k'},m} - \epsilon_{{\rm K+k'+q},n}} |D_{({\rm K+k+q})n,({\rm K+k'})m}|^2 . dk'. \quad (2)$$

KAs occur for phonons (i) having non-zero EPC between states close to the Fermi energy, and (ii) for which the denominators in Eq. 1,2 vanish, resulting in the presence of a singularity in the dynamical matrix [33]. Thus, within a static approach, the anomalies are predicted to occur for the values of q that make the denominator in Eq. 2 vanish, i.e. for $q = 0$ and $q = 2k_F$ [22, 33, 34, 35, 36].

Thus, TDPT deeply modifies the description of the KAs. Because of the $\hbar\omega_q + i\gamma$ terms, and assuming the electronic bands of the SWNTs at the Fermi energy to be linear with slope β, the denominator of Eq. 1 vanishes for $q = \pm\hbar\omega_q/\beta$ and $q = k_F \pm \hbar\omega_q/\beta$, resulting in a shift of the position of the KAs. We refer to the inclusion of these terms as the *dynamic effects*.

By using the folding approach described in Refs. [20, 22], we numerically integrate Eq. 1, 2, and obtain the theoretical description of the KAs in metallic SWNTs within the static and the dynamic approaches. These results are then corrected to account for curvature [20].

Fig. 2 shows the phonon dispersion of the LO and TO modes close to $q = 0$ for a metallic SWNT with d = 1.0 nm. Calculations are done within the static and the dynamic approaches, at room T. The first predicts a KA for the LO mode only. This is centered at $q = 0$, and the phonon dispersion close to it has a logarithmic shape. On the other hand, dynamic calculations show that both the LO and TO phonon branches are affected by KA, and that the anomalies are centered at $q = \hbar\omega_q/\beta$.

Eq. 1,2 depend on the occupation of the electronic states through the Fermi-Dirac distribution. Thus, it is possible to compute the dependence of the phonon frequencies on the electronic temperature.

To stress that these effects depend uniquely on the occupation of the electronic bands of the tubes, here we distinguish between the electronic and the ionic temperature, which we indicate with T_e and T_i respectively. T_i corresponds to the energy associated to the atoms vibrating around their equilibrium positions, and determines the onset of the an-harmonic effects, while T_e fixes the electronic states population according to the Fermi-Dirac distribution and determines the shape of the KA. At thermal equilibrium $T_i = T_e = T$.

Fig. 2 shows the KA of the LO branch for a metallic SWNT of d = 1.0 nm calculated at T_e=4K, 300K and 2000K within the static and the dynamic frameworks. In both cases, increasing T_e results in a softening of the anomaly, this being stronger if the dynamic effects are taken into account. The TO branches do not show any dependence on T_e in both the static and the dynamic approach. Thus, the static and the dynamic models predict

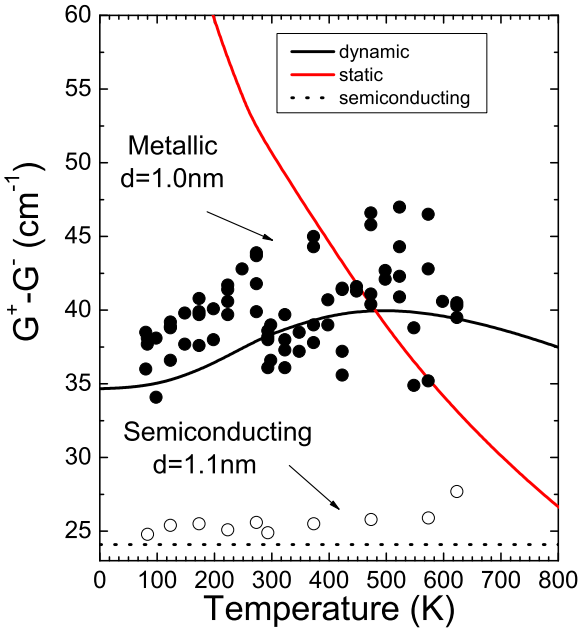

FIG. 3: Temperature dependence of the G^+ and G^- splitting compared with the theoretical prediction of the LO-TO splitting obtained using static and dynamic approaches.

a totally different temperature dependence of the splitting between the LO and the TO phonons at $q = 0$.

The LO and TO frequencies are also modified by the presence of an-harmonic effects, which are related to T_i and are expected to give an overall decrease of the phonon frequencies for increasing T. These are not described by Eq. 1,2. However, a simple model for the T dependence of the frequency shift for the LO and TO modes predicts them to be the same [37]. Thus, the *relative* position of these two modes is determined *only* by the dependence on T_e, which is entirely described by Eq. 1,2. Furthermore, since KAs affect metallic SWNTs only, no dependence of the LO-TO splitting on T_e should be observed for semiconducting SWNTs.

The experimental LO-TO splitting and those calculated by using the static and dynamic theory are plotted in Fig. 3. The static and the dynamic models give contrasting predictions. In the static case, the splitting for metallic SWNTs with $d = 1.0$ nm is estimated to be 80 cm^{-1} at 80 K, and to decrease to 50 cm^{-1} and 30 cm^{-1} at 300 K and 625 K respectively. On the other hand, the dynamic model predicts an increase of the splitting from 35 cm^{-1} to 40 cm^{-1} when moving from 80 to 520 K, and a plateau in the 420-650 K region. Both models predict a reduction of the splitting for T>650 K, with a steeper slope for the static case. For semiconducting tubes, no differences exist between the static and dynamic predictions, and the splitting for $d = 1.1$ nm is 24 cm^{-1}.

The static model trend is clearly incompatible with the experiments, which, on the opposite, are in very good agreement with the predictions of the dynamic approach. Indeed, the experimental splitting for metallic tubes shows a slight increase with temperature and peaks at $\sim$45 cm^{-1} . On the other hand, no temperature dependence is observed for semiconducting tubes, for which the splitting is $\sim$25cm^{-1}.

In conclusion, we presented the temperature dependence of the G^+ and G^- peaks in the Raman spectra of SWNTs. We showed that the temperature dependence of the G^+ and G^- splitting is significantly different in metallic and semiconducting SWNTs. The increase of the G^+ and G^- splitting in metallic tubes is due to a non-adiabatic phonon re-normalization induced by the variation in electronic temperature. This cannot be described by the standard adiabatic Born-Oppenheimer approach.

S.P. acknowledges funding from the Maudslay Society and from Pembroke College, A. C. F. from EPSRC grants GR/S97613, EP/E500935/1 the Royal Society and the Leverhulme Trust.

* Electronic address: mauri@lmcp.jussieu.fr
† Electronic address: acf26@eng.cam.ac.uk

[1] I. P. Ipatova, A. A. Maradudin, and R. F. Wallis, Phys. Rev. **155**, 882 (1967).
[2] G.E. Jellison,F.A. Modine, Phys. Rev. B **27**, 7466 (1983).
[3] M. Kuball et al., Phys. Status Solidi A **202**, 824 (2005).
[4] S. Piscanec et al., Phys. Rev. B **68**, 241312 (2003).
[5] Q. Zhang et al., Smart Mat. and Struct. **15**, S1 (2006).
[6] S. Y. Zhou et al., Nature physics **2**, 595 (2006).
[7] S. Chiashi et al., Therm. Sci. Eng. **13**, 71 (2005).
[8] Z. P. Zhou et al., Chem. Phys. Lett. **396**, 372 (2004).
[9] Y. Ouyang and Y. Fang, Physica E **24**, 222 (2004).
[10] L. Ci et al., Appl. Phys. Lett. **82**, 3098 (2003).
[11] N. R. Raravikar et al., Phys. Rev. B **66**, 235424 (2002).
[12] H. D. Li et al., Appl. Phys. Lett. **76**, 2053 (2000).
[13] F. M. Huang et al., J. Appl. Phys. **84**, 4022 (1998).
[14] C. Fantini et al., Phys. Rev. Lett. **93**, 147406 (2004).
[15] R. Krupke et al., Science, **301**, 344 (2003).
[16] R. Krupke et al., Nano Lett. **4**, 1395 (2004).
[17] H. Kataura et al., Synth. Met. **103**, 2555 (1999).
[18] H. Telg et al., Phys. Rev. Lett. **93**, 177401 (2004).
[19] A. Jorio et al., Phys. Rev. Lett. **86**, 1118 (2001).
[20] S. Piscanec et al., Phys. Rev. B **75** 035427 (2007).
[21] W. Kohn, Phys. Rev. **2**, 393 (1959).
[22] M. Lazzeri et al., Phys. Rev. B **73**, 155426 (2006).
[23] J. M. Ziman, *Principles of the theory of solids* (Cambridge University Press, London, New York, 1964).
[24] M. Born, R. Oppenheimer, Ann. Phys. **84**, 457 (1927).
[25] M. Born and K. Huang, *Dynamical Theory of Crystal Lattices* (Clarendon Press, Oxford, 1954).
[26] G. K. Horton and A. A. Maradudin, *Dynamical Properties of Solids Vol. 1* (North-Holland, Amsterdam, 1974).
[27] S. Degironcoli, Phys. Rev. B **51**, 6773 (1995).
[28] S. Pisana et al., Nature Mat. **6**, 198 (2007).
[29] M. Lazzeri,F. Mauri, Phys. Rev. Lett.**97**,266407 (2006).
[30] H. Eschrig, Phys. Stat. Sol. B **56**, 197 (1973)
[31] P. B. Allen, *Dynamical Properties of Solids Vol. 1* (North-Holland, Amsterdam, 1980).
[32] N. W. Ashcroft and N. D. Mermin, *Solid state physics*

(Saunders College, New York,London, 1976).
[33] S. Piscanec et al., Phys. Rev. Lett. **93**, 185503 (2004).
[34] O. Dubay et al. Phys. Rev. Lett. **88**, 235506 (2002).
[35] K. P. Bohnen et al., Phys. Rev. Lett. **93**, 245501 (2004).
[36] D. Connetable et al., Phys. Rev. Lett. **94**, 015503 (2005).
[37] G. Grimvall, *Thermophysical properties of materials* (North Holland, 1986)